Optical Mapping of Repolarization and Refractoriness From Intact Hearts

Igor R. Efimov, PhD; David T. Huang, MD; James M. Rendt, PhD; Guy Salama, PhD

Background Heterogeneities of repolarization (R) across the myocardium have been invoked to explain most reentrant arrhythmias. The measurement of refractory periods (RPs) has been widely used to assess R, but conventional electrode and extrastimulus mapping techniques have not provided reliable maps of RPs.

Methods and Results Guinea pig hearts were stained with a voltage-sensitive dye to measure fluorescence (F) action potentials (APs) from 124 sites with a photodiode array. AP duration (APD) was defined as the time between depolarization $(dF/dt)_{max}$ and R time points (ie, the time when AP returns to baseline or some percent thereof). However, R time points are difficult to determine because AP downstrokes are often encumbered by drifting baselines and motion artifacts, which make this definition ambiguous. In optical and microelectrode recordings, the second derivative of AP downstrokes is shown to contain an easily detected, unique local maximum. The correlation between the position of this maximum $(d^2F/dt^2)_{max}$ and R has been tested during altered AP characteristics induced by changes in cycle length, ischemia, and hypoxia. Under these various modifications of the AP, the time points of $(d^2F/dt^2)_{max}$ fell at 97.0±2.1% of recovery to baseline. Extrastimulus techniques applied to (1) isolated myocytes, (2) intact hearts, and (3) mathematical simulations indicated that $(d^2V/dt^2)_{max}$ coincided with the effective RPs of APs. The coincidence of RPs and $(d^2V/dt^2)_{max}$ was valid within 5 milliseconds, for resting potentials of −75 to −90 mV and extrastimuli three times threshold voltage.

Conclusions Thus, optical APs and $(d^2F/dt^2)_{max}$ can be used to map activation, R, and RPs with AP recordings from a single heartbeat. (***Circulation.* 1994;90:1469-1480.**)

Key Words • mapping • electrophysiology • action potentials

Spatial heterogeneities in repolarization have been proposed to explain the initiation of arrhythmias in cardiac tissue.[1] Theoretically, a unidirectional block can arise in regions containing abrupt variations of repolarization.[2] Under certain conditions, these variations can lead to wavefront fractionation and reentry. However, reliable experimental tests of this hypothesis have not been achieved.

The major obstacle to testing this hypothesis is the lack of a practical technique to measure distributions of repolarization with sufficient spatial and temporal resolution. The most common approach to map repolarization pathways is indirect, through measurements of refractory periods.[3] Maps of refractoriness are conventionally measured by combining multiple extracellular electrode recordings with premature extrastimulus techniques.[4] The heart is paced at a basic rate (S_1), and a premature stimulus (S_2) is applied with a variable coupling interval (S_2-S_1). A disadvantage of this approach is that the extrastimulus must be tested with variable delays, S_2-S_1, to determine the refractory period at each recording site and the process must be repeated at each electrode site to measure distributions of refractory periods. Maps of refractory periods derived by this approach are time-consuming and assume that the refractory period measured at one site did not vary while the measurements were repeated at other sites. As a result, such mapping measurements cannot be practically repeated under different physiological conditions without compromising both spatial and temporal resolution. Another difficulty is that the definition of refractory period depends on the amplitude, duration, and polarity of the stimulating current. Michelson et al[5] studied refractory periods in normal and ischemic myocardium and pointed out the difficulties inherent in choosing a standardized threshold current for the definition of refractory periods.

Intracellular microelectrodes provide accurate measurements of repolarization but are not practical for simultaneous measurements from multiple sites because of technical difficulty of maintaining multiple stable recordings.

Suction electrodes have been used to measure action potential (AP) durations (APDs) and refractory periods by monitoring conduction time delays between two sites.[6] Premature stimuli delivered near the relative refractory period increased conduction time delays because the extra AP propagated at slower conduction velocity. Refractory periods could thus be accurately determined and were shown to coincide with AP repolarizations. However, suction electrodes are not practical for simultaneous recordings of refractory periods at multiple sites and may produce unreliable recordings caused by tissue damage.[6]

Signal processing techniques have been proposed to estimate repolarization by use of unipolar electrograms by correlating the most rapid increase in voltage $(dV/dt)_{max}$ near the peak of the T wave to the repolarization of the local AP.[7] Millar et al[8] defined an "activation-recovery interval" as the time difference between the most rapid decrease in voltage in the QRS complex

Received January 31, 1994; revision accepted May 23, 1994.

From the Department of Cell Biology and Physiology, University of Pittsburgh (Pa) School of Medicine.

Correspondence to Guy Salama, Department of Cell Biology and Physiology, University of Pittsburgh School of Medicine, Pittsburgh, PA 15261.

$(dV/dt)_{min}$ (activation time) and $(dV/dt)_{max}$ near the peak of the T wave (repolarization time). Experimental[8] and theoretical[9] studies suggested that refractory periods were correlated with activation-recovery intervals. However, this correlation remained empirical, was strongly dependent on the shape, polarity, and kinetics of the T wave, and failed for multiphasic T waves. Ultimately, it proved to be of limited use because the amplitudes and kinetics of T waves were too variable to determine refractory periods.

We have previously used voltage-sensitive dyes and imaging technique to simultaneously measure 124 APs from the epicardium of perfused hearts.[10] In preliminary reports, we described signal processing techniques to uniquely identify the repolarization time points of fluorescence (F) APs through $(d^2F/dt^2)_{max}$ of their downstroke.[11] The algorithm was effective to measure repolarization time points even in optical AP recordings containing substantial distortions caused by movement artifacts. The method made it possible to measure heterogeneities of repolarization and APDs in normal and hypoxic hearts during abrupt cycle length shortening.[12]

The present report investigates the physiological significance of this inflection point detected during AP downstrokes by theoretical and experimental approaches. The data show that $(d^2F/dt^2)_{max}$ provides a reliable measurement of AP repolarization and is coincident with AP refractory period under physiological resting potentials. Preliminary reports of these findings have appeared in abstract form.[11,13]

Methods

Preparations

Guinea pigs of either sex weighing between 350 and 450 g were anesthetized with an intraperitoneal injection of sodium pentobarbital (Nembutal, 30 mg/kg). The hearts were rapidly excised, rapidly cannulated at the aorta (within 60 seconds), and retrogradely perfused in a modified Langendorff apparatus. The Krebs-Ringer's perfusate consisted of (in mmol/L) NaCl 130, KCl 4.75, $CaCl_2$ 1.0, $MgSO_4$ 1.2, $NaHCO_3$ 12.5, and glucose 5.0. The solution was continuously gassed with 95% O_2/5% CO_2, pH adjusted to 7.4±0.1 with $NaHCO_3$. Temperature was maintained at 35±1°C with a thermistor probe and a heat-exchange coil. A perfusion pressure of 80 to 90 cm H_2O was maintained from the beginning of the experiment with variable flow rate (≈2 $mL \cdot min^{-1} \cdot g^{-1}$ heart wt). More detailed methods describing the perfusion setup, the staining procedure, the heart chamber, optics, and computer hardware and software were previously reported[10,12,14] and are briefly restated below.

Hearts were paced at a fixed cycle length, typically 300 or 350 milliseconds, with a bipolar Ag^+/AgCl electrode placed on the epicardium. The output of the pacer was adjusted to 1.5 times the threshold voltage. A custom-designed perfusion chamber was used for studying intact guinea pig hearts. The preparation was held in place by a glass window at the front of the chamber and side and rear pads to minimize gross movement of the heart during contractions. Bipolar surface electrogram recordings were measured by use of Teflon-coated silver wires (250-μm diameter), with Ag^+/AgCl at the exposed tip of the wires and a 0.5-mm gap between the two wires. These sensing electrodes were sutured or glued to the epicardium to maintain stable recordings. The left epicardium was in contact with the glass of the front window to reduce the curvature of the ventricle and gross movement during contractions of the heart. The heart in the chamber was immersed in perfusate, which eliminated condensation on the glass window.

Staining Procedures

A styryl dye, RH-421 (S-1108, lot 2711-2, Molecular Probe), was used as the voltage-dependent fluorescent probe. When bound to the sarcolemma, RH-421 fluorescence was measured at wavelengths above the 645-nm cutoff filter when excited with a 520±20-nm interference filter. The dye exhibited a large fractional decrease in fluorescence of 6% to 9% per 100 mV depolarization such that the voltage-dependent responses appeared as upside-down APs.[14] The signals were automatically inverted under software to appear as rightside-up APs. This dye was chosen because it did not provoke detectable pharmacological effects, remained optically stable in solution, and exhibited optical APs with high signal-to-noise ratios (up to 250:1) for 2 to 4 hours.

Hearts were stained by gradual injection of 50 to 100 μL from a 3 mmol/L stock solution of dye into a 5-mL bubble trap situated directly above the aortic cannula. The final dye concentration was approximately 2.5 μmol/L, and 15 to 20 minutes was allowed for the staining to be completed. The procedure resulted in homogeneous staining throughout the heart because the dye was efficiently delivered via coronary vessels. In experiments lasting more than 4 hours, photobleaching and/or dye washout reduced the signal amplitudes; in such cases, hearts were occasionally restained to restore the original signal-to-noise ratio.

The experiments described in this study were based on a total of 20 guinea pig hearts. Six were used to map repolarization with voltage-sensitive dyes, 2 to prepare isolated myocytes for single-cell measurements of refractory periods, 6 for measurements during hypoxia, and 6 during ischemia. This investigation conformed with the Guide for the Care and Use of Laboratory Animals published by the US National Institutes of Health (NIH publication No 85-23, revised in 1985).

Instrument Setup

Details of the optical and recording apparatus have been described elsewhere.[10] The perfusion chamber containing the Langendorff-perfused heart was mounted on a micromanipulator and positioned along the optical axis of a photodiode array scanning apparatus. Light from two 45-W tungsten-halogen lamps was collimated, passed through a 520±20-nm interference filter, reflected off a 45° dichroic mirror, and focused on the left epicardium of the heart with a 35-mm camera lens (50 mm, f 1:1.4, Nikon). Epifluorescent light from the stained heart was collected, projected through a 645-nm cutoff filter, and focused to form an image of the heart on a 12×12-element photodiode array. The photodiode array consisted of 144 square diode elements, with each diode having dimensions of 1.4×1.4 mm separated by 0.1 mm of dead space. Of the 144 available diodes, 124 diodes were monitored; five elements from each corner were disregarded. The distances between the preparation, the lens, and the array could be varied and thus, the image of the heart falling on the array could be magnified by 1.5 to 6 times. In the present study, APs were recorded from a 12×12-mm^2 region of the epicardium. The depth of field of the optics restricted the detection of dye fluorescence to a depth of 144 μm from the surface of the epicardium.[14]

Signal Acquisition

A scan of data acquisition consisted of 128 simultaneously recorded traces: 124 optical plus 4 instrumentation channels. The multiplexed instrumentation channels monitored the stimulus pulses, two surface electrogram signals located on the atrium and ventricle, and in some experiments, left ventricular pressure by use of a latex balloon inserted in the left ventricular cavity and a Statham pressure transducer (model P-10). A scan consisted of a continuous recording of these 128 channels for 1.2 to 34 seconds. The photocurrents from 124 diodes were fed to a current-to-voltage converter, amplified, digitized (1.3

kHz per channel, 8 bits per sample), and stored in a memory buffer of a Digital Equipment Corp PDP 11-73 computer.

Experiments on Isolated Myocytes

Guinea pig myocytes were isolated with collagenase and pronase as previously described.[15] Current clamp measurements were performed with an Axoclamp 1D. Data were collected at a 5-kHz sampling rate. Patch pipettes were filled with a solution of the following composition (in mmol/L): KCl 140, HEPES 10, MgATP 5, EGTA 10 at pH 7.25. Cells were superfused with an external solution containing (in mmol/L): NaCl 130, KCl 5, $MgCl_2$ 1, $CaCl_2$ 2, HEPES 10, glucose 5, pH 7.35 at 37°C.

Computer Simulation

Computer simulations were performed with mathematical models of electrical activity in ventricular myocardial fiber.[16] The Beeler-Reuter model is a system of first-order nonlinear differential equations of the Hodgkin-Huxley type. To solve the system, an implicit scheme with time step $\Delta t=0.01$ millisecond was used. Activation and inactivation parameters in a model of Hodgkin-Huxley type obey the usual first-order equation

$$dy/dt=\alpha_y(1-y)-\beta_y(y)$$

where y is a parameter (m, h, etc), t is time (milliseconds), and α_y and β_y are rate constants (milliseconds). If we call y the parameter value at the nth time step (Δt), the finite-difference equation for the time derivative yields

$$(y^{n+1}-y^n)/\Delta t=\alpha_y(1-y^{n+1})-\beta_y(y^{n+1})$$

which can be rewritten to

$$y^{n+1}=(y^n+\alpha_y\Delta t)/[1+(\alpha_y+\beta_y)\Delta t]$$

The equation for membrane potential is

$$dE/dt=\Sigma i/C=\Sigma g(E-E_r)/C$$

where E is the membrane potential (millivolts), i is ionic currents ($\mu A/cm^2$), and C is the membrane capacitance ($\mu F/cm^2$). The finite-difference equation for the time derivative in this case is

$$(E^{n+1}-E^n)/\Delta t=-(1/C)\Sigma g(E^{n+1}-E_r)$$

which takes the form

$$E^{n+1}=[E^n+(\Delta t/C)\Sigma gE_r]/[1+(\Delta t/C)\Sigma g]$$

Stimulations of a model cell with normal Beeler-Reuter parameters were made by applying an external current pulse with amplitude $i_{ext}=12$ $\mu A/cm^2$ and duration $\Delta t=5$ milliseconds. Computations were performed on IBM/PC-386 clone and the CRAY C90 of the Pittsburgh Supercomputing Center. Programs were written with Borland C++ compiler.

Results

Second Derivative of the Cardiac AP

A signal-processing technique was used to detect the activation (depolarization) and recovery (repolarization) time points of fluorescence (F) APs. The activation time point was defined as the maximum first derivative $(dF/dt)_{max}$ of the AP upstroke. The recovery time point was defined as the maximum second derivative of the AP downstroke, $(d^2F/dt^2)_{max}$, because the second derivative of the cardiac AP was found to exhibit a local maximum between the most negative slope of the AP downstroke and the return to baseline.[11-13] Fig 1 illustrates the method. Fluorescence APs are first recorded from the epicardium by one of the diodes on the photodiode array (Fig 1A). The diode recorded the sum of voltage-dependent optical response of a group of cells (viewed by the diode) contained in a 1×1-mm^2 area of left epicardium and a depth of 144 μm. The recording contained high-frequency noise (Fig 1A), which was filtered with a boxcar of 8 milliseconds' duration to obtain Fig 1B. The depolarization time point of an AP recorded with an intracellular electrode is conventionally defined at the maximum first derivative of the AP upstroke, $(dV/dt)_{max}$. For optical APs, the time point of depolarization was also defined as the maximum first derivative of the fluorescence AP upstroke $(dF/dt)_{max}$ because it corresponded to the time when most of the cells viewed by a diode were depolarizing. The depolarization time point was detected by taking the first derivative of Fig 1B to obtain Fig 1C (dF/dt_{max}, at arrows). The first derivative trace (Fig 1C) was filtered with a 23-millisecond boxcar to generate Fig 1D before taking the second derivative to generate Fig 1E. The repolarization time point is typically defined as the recovery of the AP back to baseline, which provides an accurate method to measure AP duration whenever the downstroke has a large negative slope and returns abruptly to its resting potential. When the downstroke returns gradually to baseline, repolarization is alternatively defined as a percentage of recovery to baseline. These definitions are often not suitable for optical recordings because movement artifacts distort the repolarization phase (see Fig 2). Consequently, the repolarization time point was taken as the time of maximum

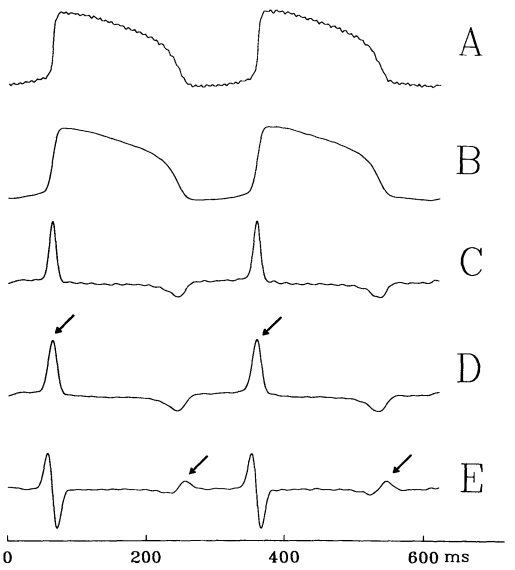

FIG 1. Tracings showing signal processing of optical action potentials (APs) to resolve depolarization and repolarization time points. A, An optical AP was recorded (at 1.3 kHz) from a 1×1-mm area of left epicardium from a perfused guinea pig heart. The voltage-dependent optical signal corresponded to a fractional decrease of fluorescence of 8%. B, The fluorescence (F) AP shown in (A) was filtered with a boxcar of 8 milliseconds' duration. C, Its first time derivative was obtained after filtration from trace B. D, Trace C was filtered with a 23-millisecond boxcar, and the time of depolarization was taken at the time point of $(dF/dt)_{max}$ of the AP upstroke (arrows on trace D). E, The time derivative of trace D is shown; note the unique peak that coincides with the end of the repolarization phase of the AP. The repolarization time point was taken at $(d^2F/dt^2)_{max}$ (arrows on trace E).

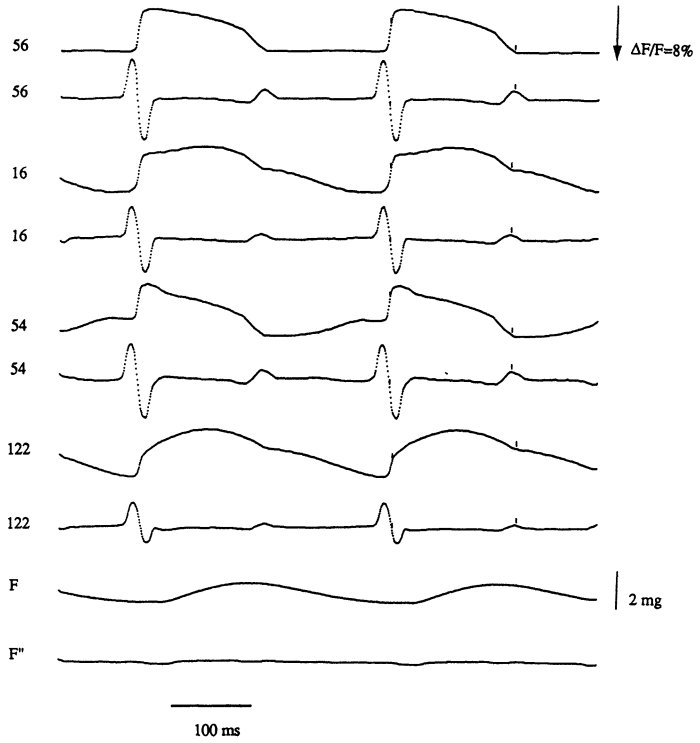

FIG 2. Tracings show that $(d^2F/dt^2)_{max}$ of action potential (AP) downstrokes are not distorted by motion artifacts. Four of 124 simultaneously recorded APs are shown, and each is followed by its second derivative determined as described in Fig 1. The AP signal from diode 56 was chosen as an example of an optical AP with negligible motion artifact. APs from diodes 16, 54, and 122 were selected for their substantial levels of motion artifacts. Their second derivatives, d^2F/dt^2, show prominent peaks at the repolarization time points of the APs. The computer algorithm automatically determined $(d^2F/dt^2)_{max}$ and placed a "tick" mark at the calculated repolarization time point. The algorithm identified unique repolarization time points for 95±2% of the APs recorded by the array. Developed force was measured with a balloon inserted into the left ventricular cavity. Peak developed force occurred during or just before the rapid phase of repolarization, and developed force was substantial during the repolarization phases, which accounted for the movement artifact. However, the second derivative of the force (and most likely movement artifacts) was relatively flat during repolarization.

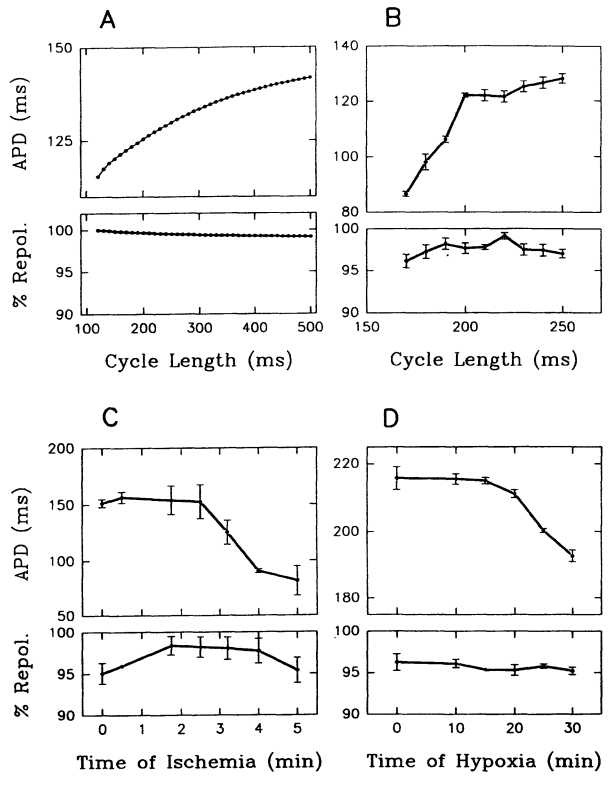

FIG 3. Graphs showing that $(d^2F/dt^2)_{max}$ coincides with action potential (AP) repolarization under various physiological and pathological conditions. The correlation between $(d^2F/dt^2)_{max}$ and repolarization was tested in simulations of the AP by use of the Beeler-Reuter model and with optical recordings under various conditions. AP durations (APD) were defined as the time difference $dF/dt_{max}-(d^2F/dt^2)_{max}$ of AP upstrokes and downstrokes. APs recorded by 12 of the 124 diodes were chosen for their negligible levels of movement artifact and were analyzed to correlate their percent repolarization (or recovery back to baseline) to the time point of $(d^2F/dt^2)_{max}$. Percent of repolarization was measured at the time point of $(d^2F/dt^2)_{max}$. For mathematical simulations, APDs were defined in the same way; that is, as the difference between $(dV/dt)_{max}$ and $(d^2V/dt^2)_{max}$. A, APs were generated from Beeler-Reuter simulations and their APDs measured as a function of cycle length (CL) (top trace). The percent repolarization at the time point of $(d^2V/dt^2)_{max}$ was determined for APs at each CL and plotted in the lower graph. The data show that as APDs increased from 115.46 to 141.71 milliseconds with CLs increasing from 120 to 500 milliseconds, the time point of $(d^2V/dt^2)_{max}$ coincided with 99.46±0.23% (mean±SD) repolarization back to baseline. B, The equivalent analysis was repeated with optical APs from the left epicardium of guinea pig hearts paced at different cycle lengths. A bipolar stimulating electrode was placed on the right atrium to pace the heart at faster rates than the intrinsic pacemaker rate. APDs from 12 central diodes were analyzed to test the correlation between $(d^2F/dt^2)_{max}$ and the percent repolarization. Top plot, Each data point represents the mean APD±SD for 12 APs recorded at a given cycle length. APDs increased from 94.09 to 130.39 milliseconds with increasing cycle lengths from 170 to 250 milliseconds. Bottom plot, Each data point represents the averaged percent repolarization±SD at the times that correspond to $(d^2F/dt^2)_{max}$ of the 12 APs; $(d^2F/dt^2)_{max}$ occurred at 96.14±0.82% repolarization (mean±SD). C and D, Same analysis as in B except that APDs and percent repolarization were plotted as a function of time of ischemia (C) and hypoxia (D). Preparations were paced at CL=350 milliseconds. Ischemia experiments were carried out at 35°C, APDs decreased from 156.52 to 81.42 milliseconds in 5 minutes of ischemia, and $(d^2F/dt^2)_{max}$ fell at 96.96±1.44% of repolarization. Hypoxia experiments were carried out at 23°C, APDs decreased from 215 to 192 milliseconds in 30 minutes, and $(d^2F/dt^2)_{max}$ fell at a similar percent repolarization of 95.67±0.43%. The higher percent repolarization in theoretical compared with the experimental results was attributed to the origins of optical signals, which represent the summed response of hundreds of cells in a patch of myocardium viewed by a diode. Experiments shown in B through D were reproduced in six hearts.

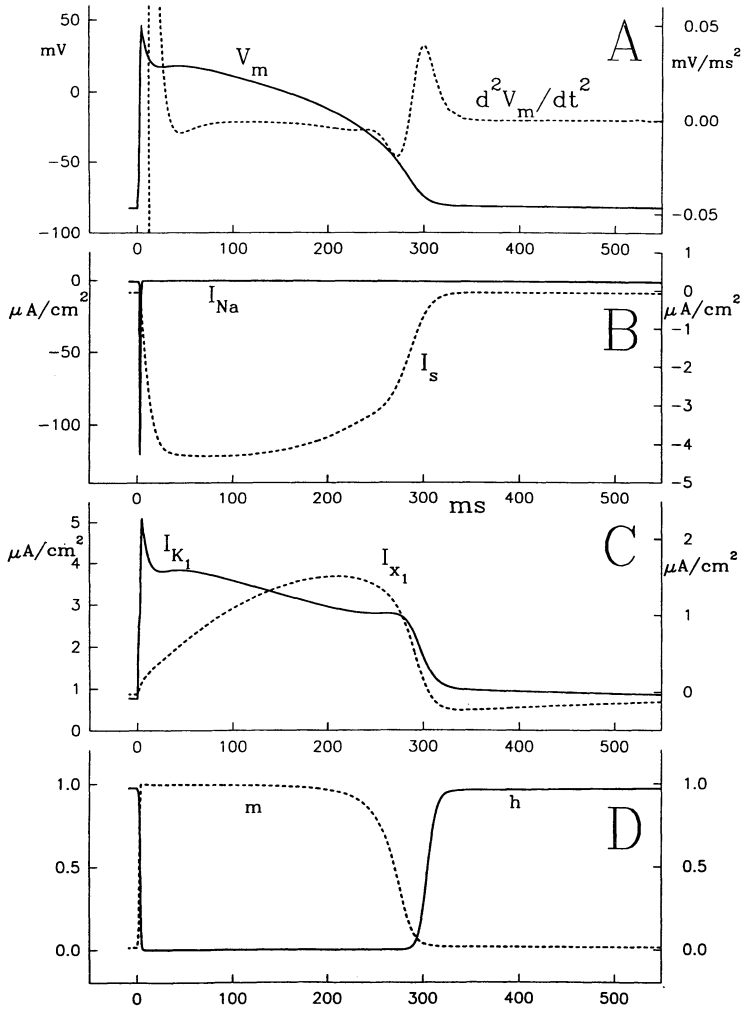

FIG 4. Plots showing Beeler-Reuter simulation of action potential (AP) and $(d^2V/dt^2)_{max}$. An AP was simulated for model guinea pig ventricular cells with a −83-mV resting potential, paced at 1 Hz. A, Superposition of the AP and its second derivative. B, Time course of the inward currents carried by voltage-gated Na^+ (I_{Na+}) and Ca^{2+} (I_S) channels. C, Time course of inward (I_{K1}) and outward (I_{x1}) rectifying K^+ channels. D, Activation (m) and inactivation (h) gates of voltage-gated Na^+ channels.

d^2F/dt^2 of the AP downstroke, a time point that fell between minimum dF/dt of the downstroke and the return to resting potential as in Fig 1E (arrows).

The second derivative of the optical AP was a particularly useful (although empirical) method to define repolarization because it identified a unique time point, even for AP downstrokes that are distorted by motion artifacts. Of 124 simultaneous AP recordings, approximately one half of the signals had negligible movement artifact, and repolarization could be determined as a percentage of recovery to baseline. For the remaining half of the APs, the return to baseline was ambiguous to various degrees because of movement artifacts. Fig 2 shows an example of an AP recording with negligible movement artifact (trace 1) followed by APs (traces 2 through 4) selected for the different kinetics of their movement artifacts. Even though the time course and direction of movement artifacts was unpredictable, we found that the second derivatives (shown below each trace) detected unique maxima that seemed independent of the movement artifact and thus appeared to identify AP repolarization time points. A possible explanation for the stable $(d^2F/dt^2)_{max}$ in the presence of movement artifacts may be the relatively slow rate of change of force (trace F) during the repolarization phase of the heart. For instance, the second derivative of the left ventricular pressure wave was constant during the repolarization phase (trace F'') and was not likely to temporally displace the voltage-dependent inflection point.

Correlation Between $(d^2F/dt^2)_{max}$ and Repolarization Time Points

The second derivative of AP downstrokes served as a useful algorithm to identify repolarization even in the presence of movement artifacts. However, to generate maps describing propagation of repolarization across the epicardium, it is important to demonstrate that $(d^2F/dt^2)_{max}$ occurred reproducibly at the same percent recovery to baseline and that changes in AP characteristics (eg, shape and/or duration) did not shift $(d^2F/dt^2)_{max}$ relative to the percent recovery. The correlation between $(d^2F/dt^2)_{max}$ and percent recovery was therefore tested under various experimental conditions and pacing frequencies. APDs from Beeler-Reuter simulations of the AP were calculated from the depolarization time point defined at $(dV/dt)_{max}$ of AP upstrokes minus the repolarization time point defined at $(d^2V/dt^2)_{max}$ of AP downstrokes. For optical APs, APDs were calculated by the same algorithm except that $(dV/dt)_{max}$ was substituted by $(dF/dt)_{max}$ and $(d^2V/dt^2)_{max}$ by $(d^2F/dt^2)_{max}$. Percent of AP recovery back to baseline was measured at the point of $(d^2V/dt^2)_{max}$ [or $(d^2F/dt^2)_{max}$] and plotted along with changes in APDs.

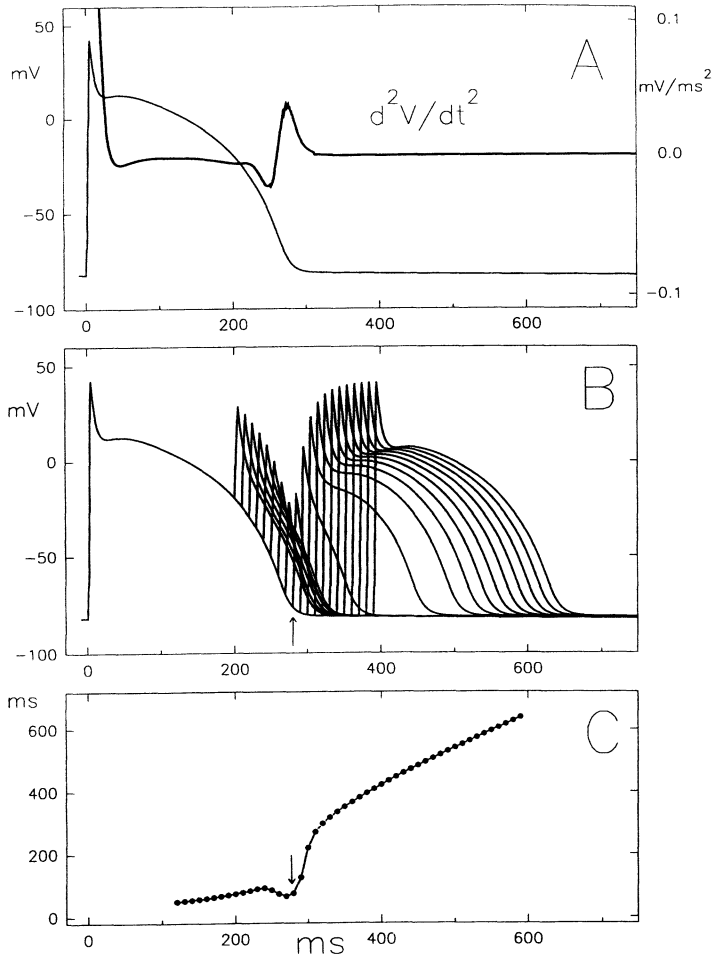

FIG 5. Plots showing refractory period predicted by the Beeler-Reuter model using premature stimuli. A, Second derivative of simulated action potential (AP) shows a prominent local maximum. B, Simulations of APs elicited by a pacing stimulus (S_1) followed by premature stimuli (S_2). Stimulations were modeled as square pulses with an amplitude of 12 $\mu A/cm^2$ (ie, 2 times threshold voltage) and a duration of 5 milliseconds. The basic cycle length (S_1) was 1000 milliseconds, and premature beats were applied once every 10 basic stimuli, at variable S_2-S_1 intervals. C, Plot of additional depolarization time induced by a premature pulse S_2 as a function of S_2-S_1 interval. The increase in depolarization time is negligible when S_2 fires during the absolute refractory period, and the total depolarization time begins to increase when S_2-S_1 is longer than 279 milliseconds (arrows), that is, when S_2 fires past the time point of $(d^2V/dt^2)_{max}$, ie, the end of the refractory period. Simulations were done on an IBM PC/386 clone computer. Integration of the equations was performed with an implicit scheme with a time step $\Delta t=0.01$ milliseconds.

The consistent correlation of $(d^2F/dt^2)_{max}$ with repolarization is illustrated in Fig 3. In Fig 3A, APDs were calculated with the Beeler-Reuter model based on $(d^2V/dt^2)_{max}$ and plotted as a function of basic cycle length (CL, in milliseconds). The simulation predicted the expected increase of APDs at longer CL and showed that $(d^2V/dt^2)_{max}$ fell in the range of 99% to 100% recovery to baseline (A, bottom plot). The longer CLs (120 to 500 milliseconds) caused significant increases in APDs from 115.46 to 141.71 milliseconds; yet, the simulation experiment predicted that $(d^2V/dt^2)_{max}$ fell at 99±0.52% of recovery for this range of APDs. Note that there was a slight decrease in percent repolarization at $(d^2V/dt^2)_{max}$, which reflected changes in AP shape at longer CLs. Microelectrode recordings of APs from isolated myocytes indicated that $(d^2V/dt^2)_{max}$ fell at 99.46±0.23% (mean±SD) of recovery (n=12 APs), which was in excellent agreement with findings from the Beeler-Reuter model. In Fig 3B, optical APs were measured from intact guinea pig hearts stained with a voltage-sensitive dye and imaged on a photodiode array. APDs increased from 94.09 to 130.39 milliseconds with increasing CL from 170 to 250 milliseconds (top), and $(d^2F/dt^2)_{max}$ fell at 96.14±0.82% of recovery to baseline. In Fig 3B, each data point represents the mean±SD of APD from a total of 12 optical APs from the center of the array. APDs were also modulated by metabolic perturbations. In Fig 3C and 3D, 24 APDs from central diodes were averaged and plotted as a function of time of ischemia and hypoxia, respectively. Ischemia induced by stopping coronary flow to the heart induced dramatic decreases in APD, from 156.52 to 81.42 milliseconds. These changes in APDs did not alter the correlation between $(d^2F/dt^2)_{max}$ and percent of recovery. That is, $(d^2F/dt^2)_{max}$ fell at 96.95±1.44% during ischemia. Hypoxia (30 minutes) induced by switching from oxygen- to nitrogen-saturated Ringer's solution decreased APDs from 215 to 192 milliseconds. Again, $(d^2F/dt^2)_{max}$ fell at 95.67±0.43% recovery to baseline. Note that this hypoxia experiment was carried out at room temperature (23°C), resulting in longer APDs (Fig 3D) compared with the other studies run at 35°C (Fig 3A through 3C). For Fig 3C and 3D, each point represented the mean APD±SEM of 124 optical APs as a function of time of ischemia or hypoxia. Fig 3B through 3D were generated from optical AP recordings with excellent signal-to-noise ratio and negligible movement artifact such that the percent recovery to baseline could be readily determined. In Fig 4A, an AP was simulated for a guinea pig ventricular cell based on the Beeler-Reuter model and the ionic currents of voltage-gated Na^+ (i_{Na^+}) and Ca^{2+} (i_s) channels (Fig 4B) and inward (i_{K1}) and outward (i_{x1}) K^+ rectifying channels (Fig 4C). The AP downstroke exhibits a maximum rate of voltage change, $(d^2V/dt^2)_{max}$, on its return to baseline (Fig 4A). The occurrence of $(d^2V/dt^2)_{max}$ is a direct consequence of the kinetics of the AP downstroke, which is controlled by

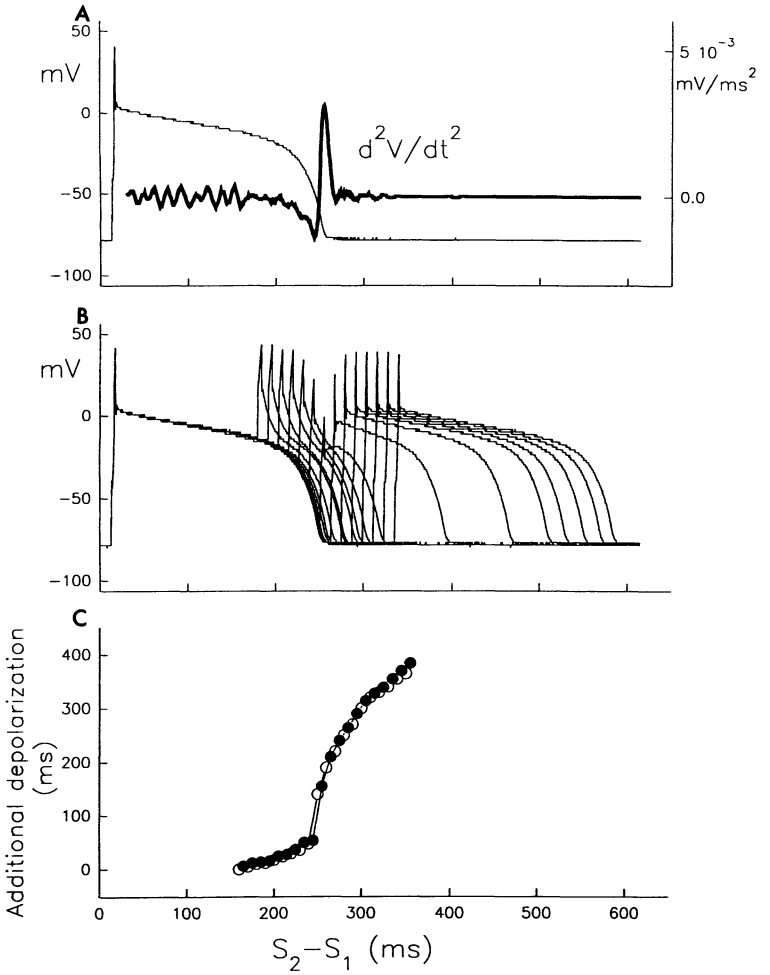

FIG 6. Plots showing that $(d^2V/dt^2)_{max}$ coincides with the refractory period of guinea pig myocytes. A, An action potential (AP) was recorded from a current-clamped guinea pig myocyte and superimposed on its second derivative. B, Extrastimuli were applied at different coupling intervals S_2-S_1 to measure the refractory period. C, Plots of AP prolongation elicited by S_2 vs S_2-S_1. When S_2 was applied before or at $(d^2V/dt^2)_{max}$, the additional depolarization time was negligible. When S_2 fired beyond the time point of $(d^2V/dt^2)_{max}$, there was a significant increase in additional depolarization time. Thus, $(d^2V/dt^2)_{max}$ coincided with the end of the refractory period. Experiments were repeated with extrastimuli of 1.5 times(filled circles) and 2 times (open circles) threshold. The results shown here were reproduced in four myocytes.

the ionic currents, primarily K^+ channels (Fig 4C), and some contribution from Ca^{2+} channels (Fig 4B). Thus, these ionic currents are also responsible for the maintained coincidence between $(d^2V/dt^2)_{max}$ and the percent recovery to baseline during alterations of AP characteristics and APDs (see Fig 3). Another important feature of $(d^2V/dt^2)_{max}$ was its close temporal relation to the recovery from inactivation of Na^+ channel h gates (Fig 4C), which suggested that $(d^2V/dt^2)_{max}$ might be coincident with the refractory period of the AP.

Correlation Between $(d^2V/dt^2)_{max}$ and Refractory Periods in the Beeler-Reuter Model

The coincidence of $(d^2V/dt^2)_{max}$ with the refractory period was investigated in the Beeler-Reuter model with programmed stimulation. A model ventricular cell was paced at a basic stimulus frequency (1 Hz) consisting of square pulses with amplitudes of 12 $\mu A/cm^2$ and durations of 5 milliseconds (S_1). The threshold to trigger an AP was 6 $\mu A/cm^2$. After 10 S_1 stimuli, a premature stimulus, S_2, with the same amplitude and duration as S_1 was delivered at different S_2-S_1 intervals. In Fig 5A, the primary AP elicited by S_1 was superimposed on the responses triggered by premature impulses delivered at different S_2-S_1 intervals. Fig 5B shows the primary AP shown in Fig 5A superimposed on its second derivative. Premature S_2 impulses prolonged the APD, thereby prolonging the total depolarization time. A plot of "additional depolarization" as a function of coupling interval (S_2-S_1) is shown in Fig 5C. As the coupling interval S_2-S_1 increased from 100 to 279 milliseconds [ie, to $(d^2V/dt^2)_{max}$], the additional depolarization time increased gradually from 50 to 87.5 milliseconds (arrows in Fig 5A and 5C). But when the coupling interval S_2-S_1 was greater than $(d^2V/dt^2)_{max}$ [ie, the premature pulse fell just beyond $(d^2V/dt^2)_{max}$], there was an increase in additional depolarization (Fig 5C), and S_2 elicited extra APs of increasingly greater amplitudes and durations (Fig 5A). This implied that $(d^2V/dt^2)_{max}$ was related temporally to the refractory period, defined as the time point when the excitable properties of the membrane are restored to fire another AP. In the Beeler-Reuter model, $(d^2V/dt^2)_{max}$ coincided with 23% recovery from inactivation (h gates) of Na^+ channels and 5 milliseconds later corresponded to >80% recovery from inactivation, which was not surprising given the steep voltage dependence of inactivation gates.

Refractory Period Coincides With $(d^2V/dt^2)_{max}$ in Isolated Myocytes

The correspondence between the effective refractory period and the maximum second derivative was examined in isolated guinea pig myocytes using microelectrode recordings and programmed stimulation. Fig 6A shows the time course of an AP and its second derivative during pacing at 1 Hz. Note that as for optical APs, electrode recordings also revealed an easily detectable

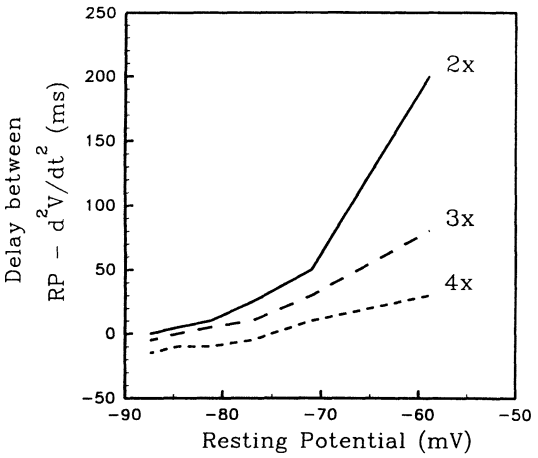

FIG 7. Plot showing that refractory periods depend on resting potential and stimulus strength. The coincidence between $(d^2V/dt^2)_{max}$ and the refractory period was tested at different resting potentials and stimulus strengths by measuring RP (the refractory period) minus $(d^2V/dt^2)_{max}$ time point. Refractory periods were measured with S_2-S_1 stimulation protocol with different stimulation strengths of 2, 3, or 4 times threshold currents and at different resting potentials. Resting potentials were varied from −88 to −58 mV by application of a constant external current. Delays between refractory period and $(d^2V/dt^2)_{max}$ were plotted as a function of resting membrane potential for extrastimuli of 2, 3, and 4 times threshold currents. At stimulus strengths of 2 and 3 times threshold and resting potentials in the range of −88 to −77 mV, the delay between refractory period and $(d^2V/dt^2)_{max}$ was within 10 milliseconds. At more depolarized resting potentials, refractory periods were longer than the repolarization of the AP, and the delay increased with weaker stimuli.

peak at $(d^2V/dt^2)_{max}$ that corresponded to the recovery of the AP back to baseline. Under these conditions, $(d^2V/dt^2)_{max}-(dV/dt)_{max}$ was 252.0 milliseconds (Fig 6A). With coupling intervals S_2-S_1 shorter than 252 milliseconds, the premature stimuli did not significantly prolong APD (Fig 6B). At coupling intervals >252 milliseconds, the extrastimulus elicited the firing of another AP, resulting in an increase in total depolarization time. In Fig 6C, the additional depolarization time was plotted as a function of coupling interval, S_2-S_1, for S_2 stimuli with amplitudes 1.5 (filled circles) and 2 (open circles) times threshold voltage. Experimental confirmation of the Beeler-Reuter model indicated that under physiological conditions, $(d^2V/dt^2)_{max}$ was coincident with the effective refractory period.

Refractory Periods Coincide With $(d^2V/dt^2)_{max}$ in a Range of Resting Potentials and Stimulus Strengths

In normally polarized ventricular muscle, $(d^2V/dt^2)_{max}$ coincided with the effective refractory period because excitability is restored rapidly on complete repolarization of membrane potential.[17] However, this relation was expected to fail in states with abnormal recovery from inactivation as described for postrepolarization refractoriness in ischemic heart muscle.[18] Prolonged refractoriness that outlasts the APD may account for rate-dependent conduction blocks and arrhythmias.[18] Another concern is that refractory periods depend on strength and polarity of test stimuli and can be shortened with increasing stimulus strength. In Beeler-Reuter simulations, the coincidence between $(d^2V/dt^2)_{max}$ and refractory periods was tested at various resting membrane potentials and strength of premature stimuli. The membrane potential was depolarized to different values (−88 to −58 mV) by constant current injections, and refractory periods were measured with premature stimuli with strengths 2, 3, or 4 times threshold. Fig 7 shows the delay between the refractory period and $(d^2V/dt^2)_{max}$ as a function of resting potential for extraimpulses 2, 3, or 4 times the threshold voltage. The plot shows that $(d^2V/dt^2)_{max}$ coincides closely with the effective refractory periods when refractoriness is tested with extrastimuli in the range of 2 to 3 times threshold voltage and for resting potentials in the range of −88 to −77 mV. For cells depolarized above −77 mV, the refractory period was considerably longer than $(d^2V/dt^2)_{max}$ or the repolarization of the AP.

The prolongation of refractory periods relative to $(d^2V/dt^2)_{max}$ was primarily due to the slower and partial recovery from inactivation of h gates at depolarized resting potentials. Fig 8 simulates the changes in ionic currents and AP characteristics when the resting potential is depolarized to −62 mV as opposed to normal resting potential (Fig 4). At a depolarized resting potential, the APD is prolonged and the maximum second derivative, $(d^2V/dt^2)_{max}$, still coincides with 99% recovery to baseline (Fig 8A). However, $(d^2V/dt^2)_{max}$ no longer coincides with the refractory period (Fig 7). In this case, the regenerative response becomes a Ca^{2+} AP since I_{Na+} becomes negligible and the dominant depolarizing current is the slow inward current I_s (Fig 8B), which persists as for APs with normal resting potential (Fig 4B). The prolongation of refractory period relative to repolarization is predominantly due to the slow and partial recovery of h-gate inactivation (Fig 8D). However, K^+ currents may also contribute to postrepolarization refractoriness because both I_{K1} and I_{x1} remain outward currents at depolarized resting potential (Fig 8C), whereas during the "resting phase" of the AP, both currents shift to inward currents at normal resting potentials (Fig 4C).

Refractory Periods in Intact Hearts Measured With Voltage-Sensitive Dyes

In multicellular preparations, refractory period is better defined as the time point when an extrastimulus can reexcite the tissue, as evidenced by an additional wave of propagating APs. The relation between $(d^2V/dt^2)_{max}$ and the effective refractory period was tested in perfused hearts by programmed stimulation. Hearts were stained with a voltage-sensitive dye and paced with a basic CL of 350 milliseconds, and every 10 basic stimuli S_1, a premature pulse S_2 was applied. Both basic and premature stimuli had amplitudes 2 times threshold voltage. The same epicardial bipolar electrode served to deliver S_1 and S_2 and was placed at the base of the left ventricle. Optical APs were recorded from a site near the location of the stimulating electrode and along the epicardium to monitor the spread of the basic and extra APs. As for the Beeler-Reuter model and single-cell experiments, the additional depolarization induced by the extra impulse was plotted as a function of coupling interval S_2-S_1. Fig 9 shows an example from one heart in which each data point represents the average prolongation of depolarization from 24 recordings of optical APs and the error bars represent the SEM. The extrastimu-

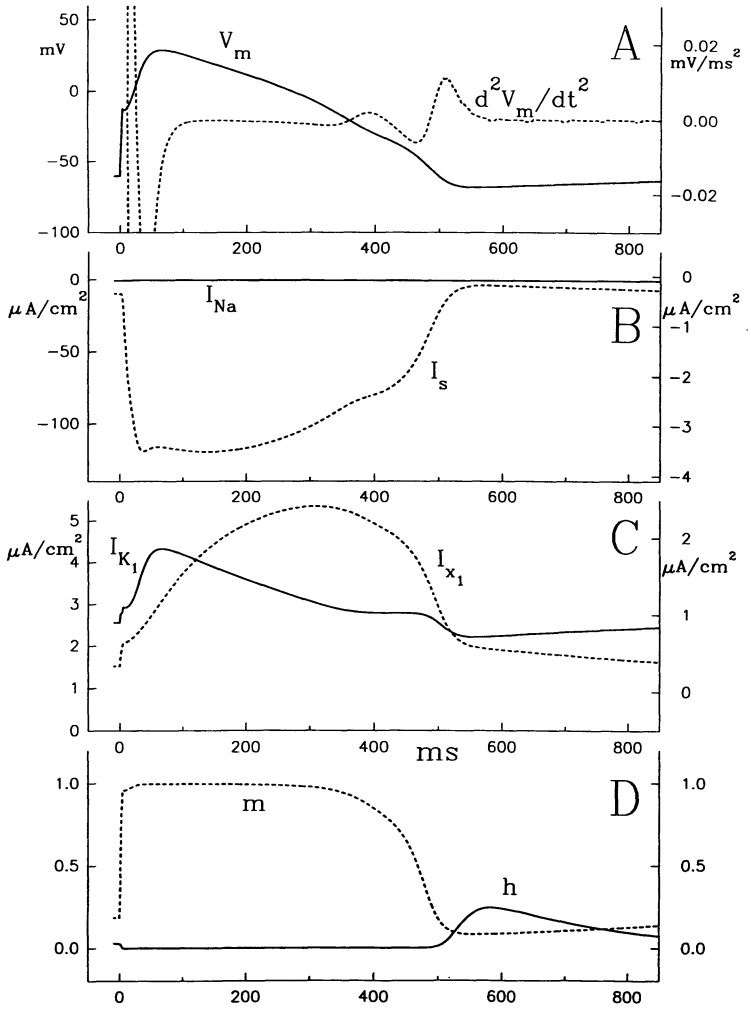

FIG 8. Plots showing simulations of action potential (AP) and ionic currents at a depolarized resting potential. The AP of a model cell was simulated as described in Fig 4, except that the resting potential was depolarized to −62 mV. A, At −62 mV, the AP is prolonged compared with −85 mV (Fig 4A) and $(d^2V/dt^2)_{max}$ coincides at 99% recovery to baseline. B, The Na^+ inward current is negligible and the slow inward current (I_s) is reduced compared with Fig 4B. C, Similarly, both the inward and outward rectifying K^+ currents are reduced at depolarized potentials. D, At $(d^2V/dt^2)_{max}$, the lack of recovery from inactivation (h) is striking.

lus protocol began with a coupling interval S_2-S_1=50 milliseconds and was increased in 25-millisecond increments. APD (220.4±4.5 milliseconds, n=24 APs or 24 photodiode signals) was determined from $(d^2F/dt^2)_{max}$ minus $(dF/dt)_{max}$ of a single AP uninterrupted by an S_2 premature impulse. If the test stimulus S_2 was applied earlier than the APD determined from the previous, uninterrupted AP [eg, earlier than the time point of $(d^2F/dt^2)_{max}$], the extra impulse initiated a small depolarization with negligible AP prolongation. Moreover, the AP shape and kinetics were not significantly altered compared with the previous AP. When S_2 fell on or beyond $(d^2F/dt^2)_{max}$ (S_2-S_1=218 milliseconds), S_2 elicited a depolarizing response with increasing amplitude and duration. Thus, the time of $(d^2F/dt^2)_{max}$ indicated the end of the refractory period, after which time point, a propagating AP can be elicited by an impulse of 2 times threshold voltage. Note that guinea pig hearts with circumferences >45 mm were found to be highly vulnerable to arrhythmias induced by a single premature extrastimulus, particularly when the premature stimulus, S_2, was applied close to the rising phase of the second derivative or to $(d^2F/dt^2)_{max}$. The induction of arrhythmias prevented us from measuring the additional depolarization when the premature stimulus, S_2, fell within 50 milliseconds of $(d^2V/dt^2)_{max}$.

Based on $(dV/dt)_{max}$ as the time point of depolarization and $(d^2V/dt^2)_{max}$ as the time point for repolarization and refractoriness, a single scan of optical APs recorded in one heartbeat could then be analyzed to map activation, repolarization, and refractoriness. In Fig 10, the heart was paced at the center of the left ventricular epicardium with a bipolar electrode, resulting in anisotropic propagation of APs (in 10 milliseconds), with a major axis aligned with the longitudinal axis of epicardial fibers (Fig 10A). Repolarization spreads systematically from apex to base (in 45 milliseconds); that is, with considerably slower propagation velocity compared with activation (Fig 10B). Heterogeneities of refractoriness had the same orientation as the repolarization patterns and differed from 146 milliseconds at the apex to 188 at the base of the heart (Fig 10C). The maximum propagation velocity of repolarization was oriented at 110° to 120° angles, close to the orientation of maximum activation velocity at a 135° angle (n=12 hearts).

Discussion

Our main findings are that the second derivative of the cardiac AP exhibits a unique maximum during the repolarization phase at a point beyond the maximum negative slope. This point of inflection can be reliably detected by signal-processing techniques. With optical recordings, $(d^2F/dt^2)_{max}$ falls at a time point on the AP that is at 96% of recovery back to baseline and can be detected despite substantial levels of motion artifact. The point of inflection can be readily detected with the Beeler-Reuter model of

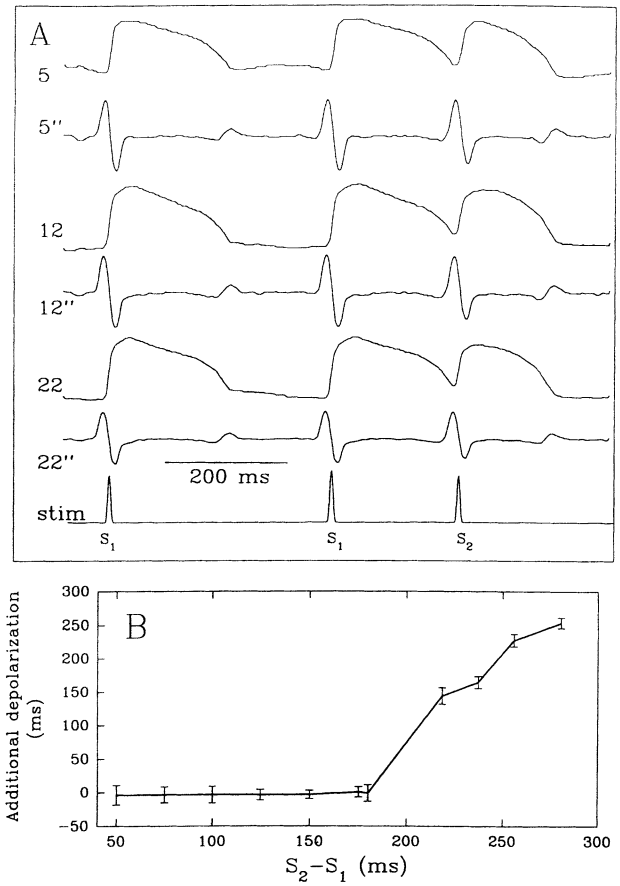

FIG 9. In intact hearts, $(d^2F/dt^2)_{max}$ coincides with the refractory period. A, Illustration of optical action potentials (APs) and their second derivative from diodes 5, 12, and 22, first during stimulation with a basic cycle length S_1-S_1=350 milliseconds, then a premature stimulus with an S_2-S_1 interval of 202 milliseconds, ie, just beyond the time point of $(d^2F/dt^2)_{max}$. B, Plot of additional depolarization as a function of coupling interval. Each data point represented the average additional depolarization from 12 patches of tissue viewed by 12 diodes on the array. When S_2-S_1 was longer than $(d^2F/dt^2)_{max}$ minus $(dF/dt)_{max}$, the extrastimulus elicited a second propagating AP, causing a striking increase in total depolarization. The data show that $(d^2F/dt^2)_{max}$ coincides with the recovery of excitability and the refractory period at various sites on the epicardium.

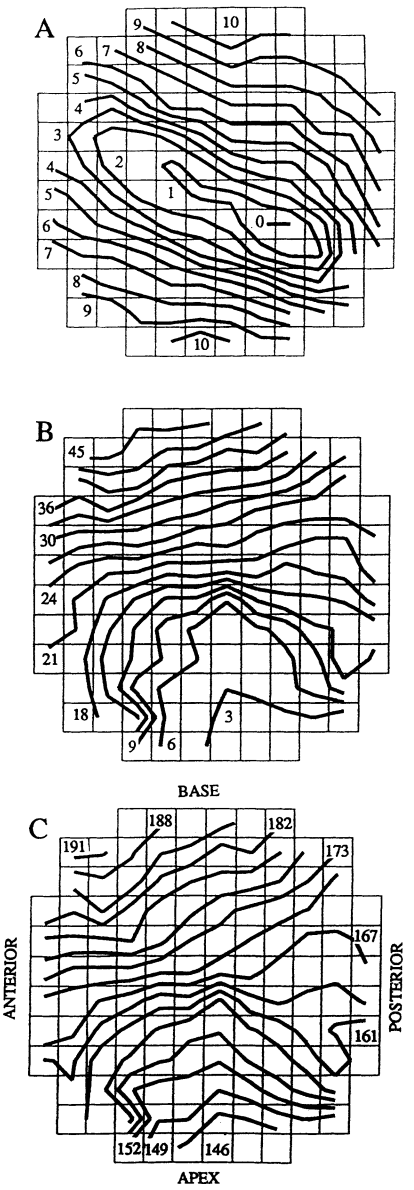

FIG 10. Optical maps of activation, repolarization, and refractoriness. A bipolar electrode was placed at the center of the left ventricular epicardium and was used to pace the heart with a basic cycle length of 300 milliseconds. Computer algorithms were used to calculate the time points of $(dF/dt)_{max}$ and $(d^2F/dt^2)_{max}$ for each action potential, then to detect the first site to depolarize and the first site to repolarize. From the time delays in depolarization and repolarization between various sites on the epicardium, activation and repolarization maps were generated and displayed as isochronal lines. A, Activation map. Activation began at the first site to depolarize, which corresponds to the location of the stimulating electrode. Activation spread anisotropically, with a major and minor axis that were parallel to the longitudinal and transverse axes, respectively, of fibers on the epicardium. The activation of the epicardium occurred in 10 milliseconds. B, Repolarization map. Repolarization began near the apex of the heart and spread systematically toward the base in 45 milliseconds. C, Maps of refractory periods. Given that $(d^2F/dt^2)_{max}$ is coincident with the refractory period, maps of refractoriness were generated from $(d^2F/dt^2)_{max}$ minus $(dF/dt)_{max}$ at each site on the epicardium. The earliest sites to recover from refractoriness (in 146 milliseconds) were located near the apex, and recovery of excitability spread toward the base, which recovered in 191 milliseconds. The orientation of the heart relative to the array is shown in C, and time delays between isochrones are labeled in milliseconds.

the AP and intracellular microelectrode recordings on single cells or multicellular preparations. In simulations and myocytes, $(d^2V/dt^2)_{max}$ falls at 99% to 100% of recovery, but with optical APs it falls at about 96% of recovery. This difference was a consequence of optical recordings consisting of the summed response of hundreds of cells contributing to a diode signal. Even when the APD was varied by manipulation of the experimental conditions, $(d^2F/dt^2)_{max}$ coincided reliably with the 96% recovery to baseline. This implied that under physiological and pathological conditions (hypoxia and ischemia), $(d^2F/dt^2)_{max}$ could be used in a practical way to map patterns of repolarization.

Detection of Refractory Periods

Besides its correlation with the repolarization time point, $(d^2V/dt^2)_{max}$ was shown to coincide with the effective refractory period of the AP, measured by conventional extrastimulus techniques. The latter finding was

not surprising, given that recovery of excitability is a rapid process once repolarization of the membrane potential is complete and the recovery from inactivation (h gates) of Na^+ channels exhibits a steep voltage dependence.[18] Although the correlation of $(d^2V/dt^2)_{max}$ and refractory period is valuable to map patterns of refractory periods, it is important to point out the limitations of this approach in depressed (ie, ischemic) myocardium. Ischemic tissue is known to exhibit prolonged refractory periods beyond the repolarization phase of the AP.[17] The prolongation of refractory periods in relation to $(d^2V/dt^2)_{max}$ was demonstrated in Beeler-Reuter simulations with increasing depolarization of the resting potential (Fig 7) and was attributed primarily to the slow and partial recovery from inactivation (Fig 8). In the present simulation experiments, resting potential was made less negative by constant current injection; this suggests that depolarization of the resting potential may be sufficient to produce postrepolarization refractoriness. Experimental studies demonstrate that heart muscle depolarized with high extracellular K^+ shares the properties of postrepolarization refractoriness seen in ischemic myocardium.[19] The predominant view is that prolongation of refractoriness is determined by a lack of regenerative inward current (I_{Na^+} and I_s) caused by a slow recovery from inactivation.[18,20] In addition, postrepolarization refractoriness induced by high extracellular $[K^+]_o$ was shown to be related, in part, to an increased K^+ conductance caused by the elevation of $[K^+]_o$ and a shift in threshold voltage to less negative potentials.[19]

The coincidence of $(d^2V/dt^2)_{max}$ and refractory period was tested and shown to be valid with extrastimuli of strengths ranging from 2 to 4 times threshold voltage. However, refractory periods depend on the strength of the extra impulse, and a definition of refractory period is necessarily linked to the method used to test for refractory periods. For instance, large defibrillating currents applied early after the upstroke of an AP overcame the absolute refractory period and elicited a second AP with shortened APD.[21] The effect of defibrillating stimuli was interpreted to prolong APDs and refractory periods because the occurrence of two successive APs prolonged the total depolarization time.[21] Thus, a definition of refractory period must specify (1) the stimulus strength, (2) whether the spread of a premature AP is a necessary condition to define the refractory period of the basic AP, and (3) whether one considers the refractory period of basic AP that was interrupted by the premature impulse or the refractory period of the "total depolarization" (ie, the basic AP plus the depolarization induced by defibrillating shocks).[21]

Real-Time Maps of Repolarization and Refractory Periods

The method proposed in this paper makes it possible to avoid most of the difficulties encountered with conventional techniques. Imaging technique and voltage-sensitive dyes combined with the detection of $(dF/dt)_{max}$ as activation and $(d^2F/dt^2)_{max}$ as repolarization time points make it possible to obtain maps of activation, repolarization, and refractory periods with high temporal and spatial resolution.

A disadvantage of imaging technique with voltage-sensitive dyes is the superposition of motion artifacts in some AP recordings. Thus, the commonly used definition of APD as a time between depolarization and the point at which AP returns to baseline or some percent thereof is difficult to determine in the case of optical APs and leads to ambiguous results. Fortunately, the local maximum peak of (d^2F/dt^2) remains undistorted even in APs containing significant levels of motion artifact. Adjacent photodiodes frequently record APs with significant differences in level and polarity of motion artifact. Nevertheless, the spatial dispersion of repolarization [measured through $(d^2F/dt^2)_{max}$] demonstrated the systematic correlation of APD and of repolarization times as a function of distance from each diode to diodes detecting APs from increasingly greater distances.[12] Thus, repolarization time points [detected by $(d^2F/dt^2)_{max}$] from ventricular epicardia under normoxic conditions resulted in the reconstruction of a systematic spread of repolarization.

The proposed techniques make it possible to measure spatial distributions of repolarization and refractoriness in intact beating hearts. Fig 10 presents an example of activation (A), repolarization (B), and refractory maps (C) measured from the left epicardium. The data show the expected anisotropic spread of activation. More interesting and novel is that the repolarization pattern is significantly different from the activation pattern. Repolarization begins at the apex and then spreads anisotropically toward the base, albeit at slower propagation velocities compared with activation. The spread of repolarization was highly reproducible (n=24) and was guided by intrinsic anisotropy of epicardial fibers on the left ventricle. In normoxic myocardium, repolarization patterns were closely correlated to maps of refractory periods, which for the first time revealed evidence for shorter refractory periods at the apex than the base. Finally, a major advantage of optical and signal processing techniques is that such maps can be generated in "real time," that is, from simultaneous recordings of APs, during a single heartbeat.

Acknowledgments

This work was supported by the Western Pennsylvania Affiliate of the American Heart Association and the Whitaker Research Foundation. Dr Efimov was supported by the National Research Council and the Pittsburgh Supercomputing Center (NSF grant DCB920011P). Dr Huang was supported by Physician Investigator Training Grant 5T32-DK07458 (National Institutes of Health). Dr Rendt was supported by a fellowship from the Western Pennsylvania Affiliate of the American Heart Association.

References

1. Moe GK, Rheinboldt WC, Abildskov JA. A computer model of atrial fibrillation. *Am Heart J*. 1964;67:200-220.
2. Reshetilov AV, Pertsov AM, Krinsky VI. Myocardial parameters controlling vulnerability: analysis of mathematical models [in Russian]. *Biofizika*. 1979;24:129-134.
3. Hoffman BF, Kao CY, Suckling EE. Refractoriness in cardiac muscle. *Am J Physiol*. 1957;190:473-482.
4. Gough WB, Mehra R, Restivo M, Zeiler RH, El-Sherif N. Reentrant ventricular arrhythmias in the late myocardial infarction period in the dog, 13: correlation of activation and refractory maps. *Circ Res*. 1985;57:432-442.
5. Michelson EL, Spear JF, Moore EN. Electrophysiological and anatomical correlates of sustained ventricular tachyarrhythmias in a model of chronic myocardial infarction. *Am J Cardiol*. 1980;45:583-590.

6. Avitall B, Naimi S, Levine HJ. Prolongation of the conduction time of early premature beats: a marker of ventricular action potential duration. *Am Heart J*. 1988;116:1247-1252.
7. Wyatt RF. Comparison of estimates of activation and recovery times from bipolar and unipolar electrograms to in vivo transmembrane action potential durations. *Proc IEEE Eng Med Biol Soc*. Piscataway, NJ: Institute of Electrical and Electronic Engineers; 1980:22-25.
8. Millar CK, Kralios FA, Lux RL. Correlation between refractory periods and activation-recovery intervals from electrograms: effects of rate and adrenergic interventions. *Circulation*. 1985;72: 1372-1379.
9. Steinhaus BM. Estimating cardiac transmembrane activation and recovery times from unipolar and bipolar extracellular electrograms: a simulation study. *Circ Res*. 1989;64:449-462.
10. Salama G, Lombardi R, Elson J. Maps of action potential and NADH fluorescence in intact working hearts. *Am J Physiol*. 1987; 252:H384-H394.
11. Salama G, Rosenbaum DS, Kanai T, Cohen RJ, Kaplan DK. Measuring spatial inhomogeneities in action potential duration and repolarization using optical transmembrane potentials. *Proc IEEE Eng Med Biol Soc*. Piscataway, NJ: Institute of Electrical and Electronic Engineers; 1989;11:222-223.
12. Rosenbaum DS, Kaplan DT, Kanai A, Jackson L, Garan H, Cohen RJ, Salama G. Repolarization inhomogeneities in ventricular myocardium change dynamically with abrupt cycle length shortening. *Circulation*. 1991;84:1333-1345.
13. Efimov IR, Huang DT, Rendt JM, Salama G. Mapping of refractory periods with voltage-sensitive dyes. *Proc IEEE Eng Med Biol Soc*. Piscataway, NJ: Institute of Electrical and Electronic Engineers; 1993;15:703-704.
14. Salama G, Kanai A, Efimov IR. Subthreshold stimulation of Purkinje fiber interrupts ventricular tachycardia in intact hearts. *Circ Res*. 1994;74:604-619.
15. Mitra R, Morad M. A uniform enzymatic method for dissociation of myocytes from hearts and stomachs of vertebrates. *Am J Physiol*. 1985;249:H1056-H1060.
16. Beeler GW, Reuter H. Reconstruction of action potential of ventricular myocardial fibers. *J Physiol*. 1977;268:177-210.
17. Lazzara R, El-Sherif N, Scherlag BJ. Disorders of cellular electrophysiology produced by ischemia of the canine His bundle. *Circ Res*. 1975;36:444-454.
18. Gettes LS, Reuter H. Slow recovery from inactivation of inward currents in mammalian myocardial fibers. *J Physiol (Lond)*. 1974; 240:703-724.
19. Rozanski GJ, Jalife J, Moe GK. Determinants of postrepolarization refractoriness in depressed mammalian ventricular muscle. *Circ Res*. 1984;55:486-496.
20. Kohlhart M, Krause H, Kubler M, Herdey A. Kinetics of inactivation and recovery of the slow inward current in the mammalian ventricular myocardium. *Pflugers Arch*. 1974;355:1-17.
21. Dillon MS. Optical recordings in the rabbit heart show that defibrillation strength shocks prolong the duration of depolarization and the refractory period. *Circ Res*. 1991;69:842-856.